2016

An Analytical Model of Rainfall Interception by Urban Trees

FINAL REPORT

JIE YING (JENNY) HUANG

MASTER OF LAND AND WATER SYSTEMS (MLWS)

THE UNIVERSITY OF BRITISH COLUMBIA

Table of Contents

List of Tables

List of Figures

List of Glossary

BAI = Bark Area Index

c = Canopy Cover

$\bar{E}/\bar{R}$ = Ratio of evaporation rate to rainfall rate during saturated canopy conditions (dimensionless)

I_a = Interception loss during canopy drying (mm)

I_c = Interception loss during canopy wetting for $P_G < P_g$ (mm)

I_{net} = Net interception loss (mm)

I_s = Interception loss during saturated canopy conditions (mm)

I_w = Interception loss during canopy wetting for events $P_G \geq P_g$ (mm)

LAI = Leaf Area Index

k = Extinction Coefficient

p = Direct throughfall proportion (dimensionless)

P_G = Gross rainfall (mm)

P_g = Gross rainfall required to saturate the canopy (mm)

Q = Solar radiation ($J/m^2/s$)

S = Saturation storage of the crown (mm)

S_L = Specific Leaf Storage

S_b = Specific Bark Surface Storage

T = Free throughfall (mm)

T_a = Air temperature (◦C)

μ = Wind speed ($m\ s^{-1}$)

Executive Summary

Urban growth and development have led to the loss of many vegetated areas and replaced them with impervious surfaces. Trees play critical roles in regulating the hydrological cycle and affecting surface water in the urban environment. They help to reduce stormwater runoff generation by intercepting, infiltrating, and evaporating significant amounts of rainwater. Research has investigated the environmental, economic, and social benefits of urban trees, among which significant economic benefits were identified in stormwater management and flood control associated with rainfall interception by urban trees. Using urban trees is one effective stormwater source control approach, yet not many new urban developments have actively utilized trees on or adjacent to a property in a rainwater management plan.

This project provides an analytical model on rainwater interception performance of a selection of common urban tree species in the Metro Vancouver area, given a series of climatic conditions and tree characteristics. The two steps of data inputs in this model include the input of meteorological data to allow calculation of evaporation rate, and the input of leaf area index values for the species of interest. The outcome of the model is intended to support the implementation of rainwater management plans in the District of North Vancouver. By generating the amount of rainfall intercepted by different tree species, the model potentially provides useful information to address several aspects of urban stormwater management for different stakeholders, such as city/municipal planners, engineers, developers, and local decision makers.

This report presents the benefits of urban trees and the rainfall interception processes and potential application of the model. The model performance is evaluated by comparing modelled data and measured data, as well as through a sensitivity analysis. Four common planted street trees including White Oak (*Quercu alba L.*), Norway maple (*Acer platanoides L.*), Green ash (*Fraxinus pennsylvanica Marsh*.), and *Prunus.spp*. were tested in the model to see how their interception performance varies. The interception performance for selected species under projected climate scenarios is also demonstrated. Lastly, the report identifies the limitations of the model, and this is followed by the author's recommendations for model users.

Overall, this model performed with a reasonable capacity to simulate canopy interception loss. The key findings were:

- The comparison results show that this rainfall interception model slightly underestimates the interception loss. The discrepancy between modelled data and actual observations could be the result of a series of factors, such as air temperature, wind speed, relative humidity, leaf area index, and rainfall rate.
- The three key parameters in this model: evaporation rate to rainfall rate ratio, free throughfall coefficient, and crown storage capacity, have different degrees of influence on the model performance. The results demonstrate that the model is most sensitive to the evaporation rate to rainfall rate ratio.
- The four selected deciduous tree species show similar seasonal variation in rainfall interception. Among the four deciduous tree species, White Oak showed the highest capacity in intercepting rainfall over the study period, followed by Norway maple. Minimum differences were observed between Green ash and *Prunus. spp.*
- As rainfall interception is influenced by a combination effects of many factors, the predictions of future interception performance on selected species do not show clear trends and patterns with the changes of temperature data.

Several recommendations for model implementation and future research include:

- Among the three key parameters, efforts should be prioritized on obtained the evaporation rate to rainfall rate ratio.
- Measure leaf area index of target tree species as this value varies in different urban environments and the ages of trees, even for the same tree species.
- Specify foliage months for each species by utilizing high-resolution remote sensing images, which could provide a relatively accurate match with ground observations regarding the detection of green-up dates.

Chapter 1 - Introduction

Urbanization alters the natural soil profile, increases impervious surface areas and decreases vegetation cover. The losses of vegetation cover and the increase of impervious surfaces, such as roads, sidewalks, concrete buildings, and parking, result in increasing stormwater runoff, degrading water quality and impairing aquatic habitats (Asadian and Weiler, 2009). Consequently, these disruptions change the urban hydrological cycle and pose challenges to stormwater management in urban areas. With future population growth and climate change, there will be more intensified urbanization competing for land uses and more climate variability making extreme events such as drought and floods less predictable. Urban trees play critical roles in regulating hydrological cycles and affecting surface water in the urban environment. They affect all hydrologic processes as well as the spatial and temporal redistribution of moisture (Xiao and McPherson, 2003). In particular, the interception of rainfall by urban trees is a major component of the surface water balance. The canopy rainfall interception changes the urban runoff process by buffering the rainfall intensity and reducing the volume of water reaching the ground via water storage within the canopy surface (Sanders, 1986; Xiao and McPherson, 2003). The evaporation of intercepted water from tree canopies further reduces the amount of rainwater entering the soil profile, and the extension of the tree root system increases macropores that facilitate soil infiltration of water. Therefore, urban trees decrease peak flows and the total amount of urban runoff and reduce the potential damage caused by stormwater. This study models the potential rainfall interception performance of different urban tree species in the District of North Vancouver to support rainwater management plans in the area.

1.1 Benefits associated with Urban Trees

1.1.1 Environmental and Economic Benefits

Urban trees have been considered as a tool to help reduce stormwater runoff generation by intercepting, infiltrating, and evaporating significant amounts of rainwater. If improperly designed, new urban developments will lead to an increase of impervious surface areas, which will be responsible for an increasing amount of stormwater runoff. Strategic tree planting and maintenance of existing street trees can decrease stormwater runoff. It has been estimated that the annual benefit

of avoided stormwater treatment and flood control costs associated with rainfall interception of urban trees in California was $41.5 million US dollars (McPherson et al., 2016). Furthermore, the annual value per street tree of services was reported from $3.78 (McPherson and Simpson, 2002) to as high as $29.91 (McPherson et al., 2016) in some cities in the United States. In addition to regulating the urban hydrological cycle, urban trees also benefit the environment in terms of sequestering carbon, improving air quality, and reducing energy consumption by providing shade. A recent survey in the State of California found that the average annual per tree management expenditure is $19, and the benefit is $110.63, thus a value of $5.82 in benefit is returned for every $1 spent (McPherson et al., 2016). A similar return on urban tree investment was reported as $5.60 in New York (Peper et al., 2007). Trees are becoming key components of urban green infrastructure.

1.1.2 Social Benefits

In addition to environmental and economic benefits, trees and green spaces in urban environments also provide benefits to human health and well-being. For example, trees' role in filtering air is critical to support the physical health of humans. Street trees are estimated to remove 0.29kg/year of air pollutants (e.g. volatile organic hydrocarbons [VOCs], NO_2, SO_2, PM_{10}) from the atmosphere (McPherson et al., 2016). Research also suggests that access to nature has positive psychological impacts and can be part of an effective strategy to prevent mental ill health (Maller et al., 2006; Nesbitt et al., 2015). Moreover, improved community cohesion was also identified as a key social benefit of urban trees by creating a sense of place, a local identity and a system of landmarks (GreenBlue Urban, 2016). Maas et al. (2009) found that "greenness" within one km had a positive effect on social well-being. Green spaces provide recreational opportunities and aesthetic benefits, as well as help residents develop a sense of community and attachment to neighbourhoods, increase social contacts and decrease the feelings of social isolation, which can all contribute to a greater sense of social well-being (Nesbitt et al., 2015).

1.2 Rainfall interception

Rainfall is intercepted by the tree crown surface, and some raindrops directly pass through gaps between leaves and the stem, reaching the ground as free throughfall. Rainwater intercepted by tree leaves and branches is temporarily stored on leaf and bark surfaces. Eventually, this stored

water evaporates into the atmosphere, or flows down the trunk to the ground as stemflow, or drips from the leaf surfaces to the ground as throughfall.

1.2.1 Factors affecting Interception Loss

Compared to other benefits associated with urban trees, relatively few investigations have focused on the influence of urban trees on rainfall interception and stormwater runoff reduction. Many previous studies have investigated the interception loss in continuous trees stands or forest communities (Bryant et al., 2005; Pereira et al., 2009; Murakami, 2007), while only a few studies have looked at the interception loss of trees in the urban environment (Xiao et al., 2000; Asadian and Weiler, 2009).

Trees in urban areas are exposed to a different environment compared to trees in the forest. The factors affecting interception performance of trees in urban environments, such as wind speed, evaporation rate, rainfall distribution, and leaf area index (LAI) are different from those in natural forests (Xiao et al., 2000). For example, the storage capacity of the tree crown will be impacted by the leaf area index (LAI), which characterizes the plant canopy quantity by measuring one green leaf area per unit ground surface area. LAI differs among species and seasons and has significant impacts on processes such as photosynthesis, respiration, rainfall interception, and evaporation (Asadian and Weiler, 2009). Deciduous trees lose their leaves during winter seasons, thus allowing a significant amount of throughfall, while conifers would intercept some rainwater during the winter seasons because they maintain their leaves (Asadian and Weiler, 2009). It was reported that the average canopy interception for *Pseudotsuga menziesii* (Douglas-fir) and *Thuja plicata* (Western red cedar) in the District of North Vancouver, British Columbia was 49.1 and 60.9%, respectively (Asadian and Weiler, 2009), and interception by the street and park trees in Santa Monica, California ranged from 15.3% for a small *Jacaranda mimosifolia* to 66.5% for a mature *Tristania conferta* (Xiao and McPherson, 2003).

Distinguishing the potential rainfall interception performance by different species in the urban environment is significant, as it provides information to support tree selection and the decision-making process for the design of new urban developments, as well as to determine the potential monetary values associated with different tree species. Studies that differentiate the performance of rainfall interception on different species are relatively few. Thus, it is important to adapt the

previous studies that focused on interception loss in forest communities to allow a better understanding of the interception process of trees species in the urban environment, as well, to distinguish the potential performance among different tree species.

1.2.2 Applying the Interception Model

Currently, the District of North Vancouver is managing and working to mitigate risks due to climate change. Stormwater management is amongst their key concerns. Using urban trees is one effective stormwater source control approach, yet not many new urban developments have actively utilized trees on or adjacent to a property in a rainwater management plan. A rainfall interception model will benefit new urban developments by providing critical information to help urban planners and stormwater managers. This model builds upon two key works: 1) a previous rainfall interception model that was applied in a forest community (Gash, 1979; Link et al., 2004), and 2) field research that investigated the interception loss of a variety of tree species in the District of North Vancouver (Asadian and Weiler, 2009). The outcome of the model is intended to support the implementation of rainwater management plans in the District of North Vancouver. The results generated from this model may be used to inform and enhance decision support tools, such as the Water Balance Model Express (Water Balance Model, 2016), which is an interactive tool to help determine the water balances of local property developments and provide useful information for different stakeholders in planning future development. Such a tool is critical to the development of stormwater management plans and permit applications for many urban development projects in the District of North Vancouver. By generating the interception loss for different species, this model offers various options in selecting tree species with supported data, which could be utilized as additional components to enhance the Water Balance Model Express. The model also projects interception loss under different future climatic scenarios. The potential audiences who will benefit from the outcomes of this study are people involved in urban planning and management of stormwater such as city/municipal planners, engineers, developers, and local decision makers.

1.3 Objectives

This study is aimed at providing an analytical model of rainwater interception performance of a selection of common urban trees in Metro Vancouver, given a series of climatic conditions and tree characteristics. The model outputs and interface are designed to inform and enhance decision support tools, such as the Water Balance Model Express, used in the development of stormwater

management plans and permit applications associated with urban development projects (in the District of North Vancouver, and potentially other municipalities). Specific goals of this study include: (1) developing the rainfall interception model with different approaches to deriving model parameters; (2) validating the model with empirical data; (3) evaluating the sensitivity of major model parameters; (4) investigating the seasonal rainfall interception performance of four deciduous tree species; and (5) projecting future interception performance of selected tree species under climate change scenarios.

1.4 Paper Outline

Details of the interception model are presented in Chapter 2, which will start with an overview of the study site where the model is applied, followed by the methodology, which includes the model theory, derivation of parameters and data requirements, and the interception calculation. In Chapter 3, the results of an evaluation of model performance are illustrated. These will include: a comparison between modelled data and measured data, and the outcomes of a sensitivity analysis for each of the key parameters. Chapter 4 discusses the results of the investigation on four selected tree species. Starting with a brief overview of meteorological data for the study period, the inter-species variation in interception loss is presented in the form of the cumulative sum and monthly averaged interception for each rainfall event. The prediction of future interception performance for selected species is demonstrated in the last section of Chapter 4. Chapter 5 identifies the limitations of the model and this is followed by the author's recommendations for model users. A summary of key findings and the next steps for study are presented in Chapter 6.

Chapter 2. Interception model

2.1 Study Site

This project focuses on the District of North Vancouver (DNV), which is located within the Regional District of Metro Vancouver (Figure 1). The elevation of urban areas in the DNV ranges from 0 - 200 masl. The DNV is surrounded by the Coast Mountains to the North, Burrard Inlet to the south, Capilano River to the west, and Indian Arm to the east. The annual precipitation ranges from 1200mm to 3000mm depending on the elevation, and the average annual temperature is about 10°C at sea level.

Figure 1. Map of the District of North Vancouver, BC.

2.2 Rainfall Interception Calculation Methods

2.2.1 Model Theory

By definition, interception is part of rain that falls on the vegetation and evaporates without reaching the ground, and is expressed by equation (1):

$$I = P - T \tag{1}$$

where I is the interception (mm), P is precipitation, and T is the throughfall and stemflow (mm), which equals to rainfall underneath or inside the canopy (Klaasen et al., 1995).

When rainfall begins, throughfall (T; in mm) is part of rainfall that directly reaches the ground without touching the leaves and branches. The amount of direct T reaching the forest floor is represented by a free throughfall coefficient (p). T will increase approximately linearly with precipitation (P_G; in mm) at a constant rate <1, until the canopy is saturated (Figure 2). For a single rainfall event, the amount of throughfall before saturation is given by (Gash, 1979):

$$T = pP_G, \qquad P_G < P_g \tag{2}$$

The remaining part (1- p) may be temporarily stored on the canopy, evaporated into the atmosphere (E; in mm/h) or drained to the forest floor (D; in mm/h) (Klaasen et al., 1998). The parameter p is

often assumed equal to one minus the canopy cover (c), which is a measure of the fraction of the landscape covered by vegetation (Gash et al., 1995).

Once the accumulated precipitation required to saturate the canopy (P_g) is reached, the slope of the T vs. P_G plot is larger than before saturation but still <1, because evaporation is occurring during the rainfall; otherwise, the slope will be unity if there is no evaporation (Link et al., 2004). Thus, for a rainfall P_G greater than P_g, T as given by (Gash 1979) is:

$$T = pP_g + (1 - \frac{\bar{E}}{\bar{R}})(P_G - P_g), \qquad P_G \geq P_g \tag{3}$$

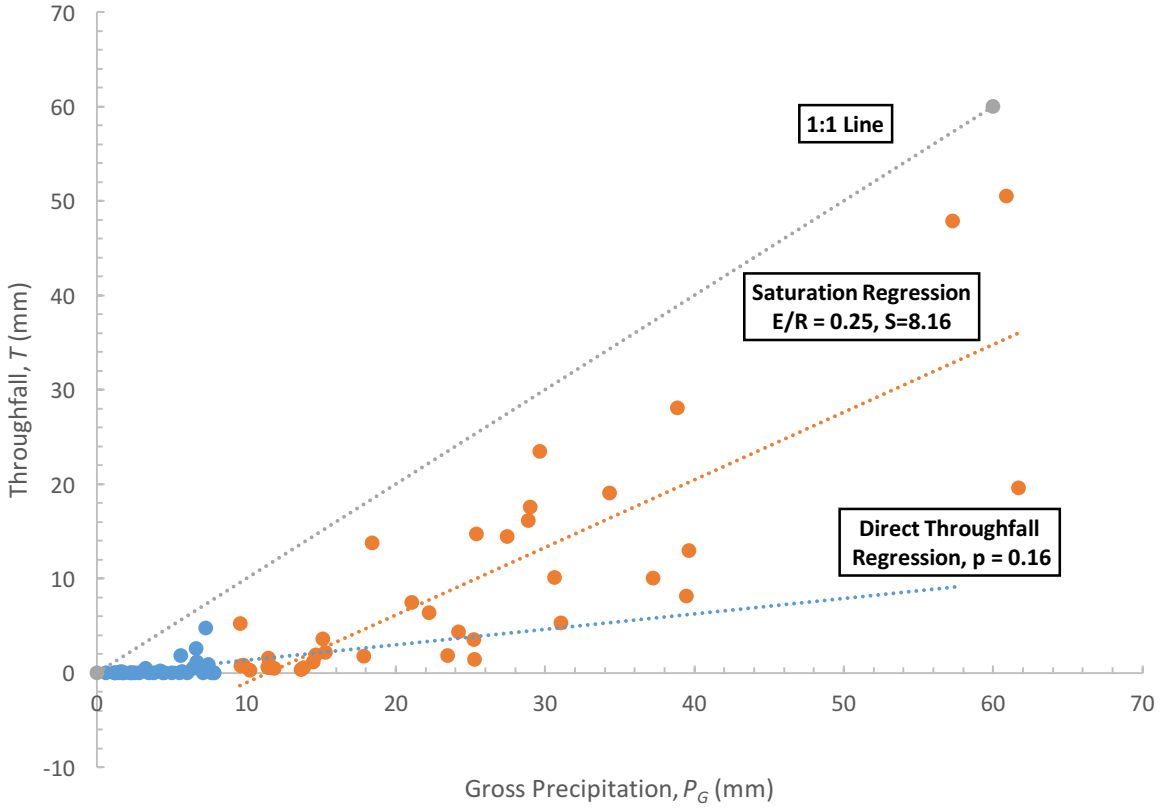

Figure 2. Example plot of data used to determine the free throughfall coefficient and the saturation storage capacity, and evaporation rate to rainfall rate ratio. The data shown is the throughfall of a single Douglas-fir tree obtained by Asadian and Weiler (2009).

By plotting the relationship between T and P_G, the main parameters of the model to be used in this study (i.e. p, $\bar{E}/\bar{R}$, S, the canopy water storage capacity) can all be estimated using the Leyton method (1967). The throughfall coefficient p is the slope of direct throughfall regression in Figure

2, $\bar{E}/\bar{R}$ is determined by the slope of saturation regression, and S is determined by the intercept of the saturation regression (Figure 2). For this study, different approaches were applied in obtaining these parameters without measuring throughfall, as one of the purposes for modelling rainfall interception is to avoid some field measurements.

2.2.2 Derivation of Parameters and Data Requirements

When no throughfall measurements were made, this analysis may be used to obtain each of the parameters by the following approaches. The mean evaporation rate ($\bar{E}$) was calculated using the Penman-Monteith equation (Appendix A) with sufficient inputs of meteorological data. Specifically, daily air temperature, relative humidity and wind speed were obtained from Environment Canada during the study period of December 2007 to November 2008 (Environment Canada, 2015), and daily solar radiation for the same period were obtained from NASA (National Aeronautics and Space Administration, 2016). The rainfall event data, including total rainfall and duration over the study period, were obtained from Asadian and Weiler (2009), who used tipping buckets rain gauges to measure the rainfall and throughfall of urban trees in the DNV. The average rainfall rate ($\bar{R}$) was then calculated by dividing gross precipitation by the duration of the rainfall event.

The two canopy parameters p and S were estimated through the LAI of specific tree species based on Equations (4) and (5).

$$c = 1 - \exp(-k*LAI) \quad (4)$$

$$S = S_L*LAI + S_b*BAI \quad (5)$$

As mentioned above, p is often assumed equal to one minus c (Gash 1995), which could be determined by its relationship to LAI (Equation 5). k is an extinction coefficient, which has ranged between 0.6 and 0.8 in forests (Ross, 1975). A value of 0.7 was set as the default value for k in the model. Specific LAI for each tree species was obtained from McPherson et al. (1994), who provided a list of LAIs for the common street tree species in Chicago, USA.

Canopy storage capacity (S) is assumed to be linearly related to LAI (Liu, 1998; Wang et al., 2008). Thus, the relationship between S and LAI is expressed as equation (5), where S_L (m) denotes the specific leaf storage, which is the maximum depth of water retained by the leaves of a particular

species per unit leaf area (Tobón Marin, 1999). Similarly, S_b (m) denotes the specific bark surface storage, which is the maximum amount of water retained by the stem and trunk of a particular species per unit area (Liu et al., 1998). Bark area index (BAI) represents the average interception storage capacity of the tree branches and trunk (Wang et al., 2008). The value of S_L was set to be 0.0002m based on reported values applied in a similar study (Wang et al., 2008). Specific BAI and S_b values were obtained from Liu et al. (1998).

Seasonal variation of LAI is necessary to be considered, as it changes S and p. For deciduous species, the LAI reaches maximum during the summer, minimum during winter (dominated by BAI), and experiences the transition process between leaf-on and leaf-off during spring and fall, respectively. For model simplification, 80% of leaf-on values for both spring and fall were assumed. The LAIs obtained from McPherson et al. (1994) were assumed to be the summer values for each selected tree species, and the summer LAIs also served as the basis of spring and fall LAI calculations. Table 1 summarizes the data inputs and the sources used in the model.

Table1. Summary of data inputs for the District of North Vancouver rainfall interception model.

Inputs	Outputs	Equations	Data Sources
Meteorological Data			NASA: http://power.larc.nasa.gov/cgi-bin/hirestimeser.cgi Environment Canada: http://climate.weather.gc.ca/historical_data/search_historic_data_e.html
Solar radiation (Q, mm/h) Air temperature (T, ℃) Relative humidity (RH, %) Wind speed (μ, m/s)	Averaged evaporation rate ($\bar{E}$)	Penman-Monteith equation	
Gross rainfall rate (R, mm) Duration of rainfall event (h)	Averaged rainfall rate ($\bar{R}$)	$\bar{R}$ (mm/h) = R/h	Empirical measurements (Asadian and Weiler, 2009)
Crown Parameters			
LAI	c S (mm)	Eqs.4 (p = 1- c) Eqs.5	McPherson et al. (1994)

2.2.3 Interception Calculation

This rainfall interception model is derived from the original Gash analytical model (Gash, 1979) and the calculations of interception components are based on Link et al. (2004), who investigated the dynamics of rainfall interception processes. The Gash analytical model (1979) is a storm-based interception model assuming rainfall is a succession of discrete storms, separated by periods long enough to allow the canopy to dry completely. Each of the discrete storms comprises three distinct phases: (1) the canopy wetting-up from the beginning of rainfall until saturation is reached; (2) the canopy is completely saturated; and (3) starting at the end of the rainfall and lasting until the trunks and the canopy are completely dry (Gash, 1979). Stemflow was also included in the calculation of Gash's model. In this project, stemflow is assumed to be negligible (Link et al., 2004), but the storage associated with branches and trunks were considered in total rainwater storage (S) by applying documented branches and stem storage capacity and surface area for each tree species as described earlier (Liu et al., 1998; Xiao and McPherson, 2016).

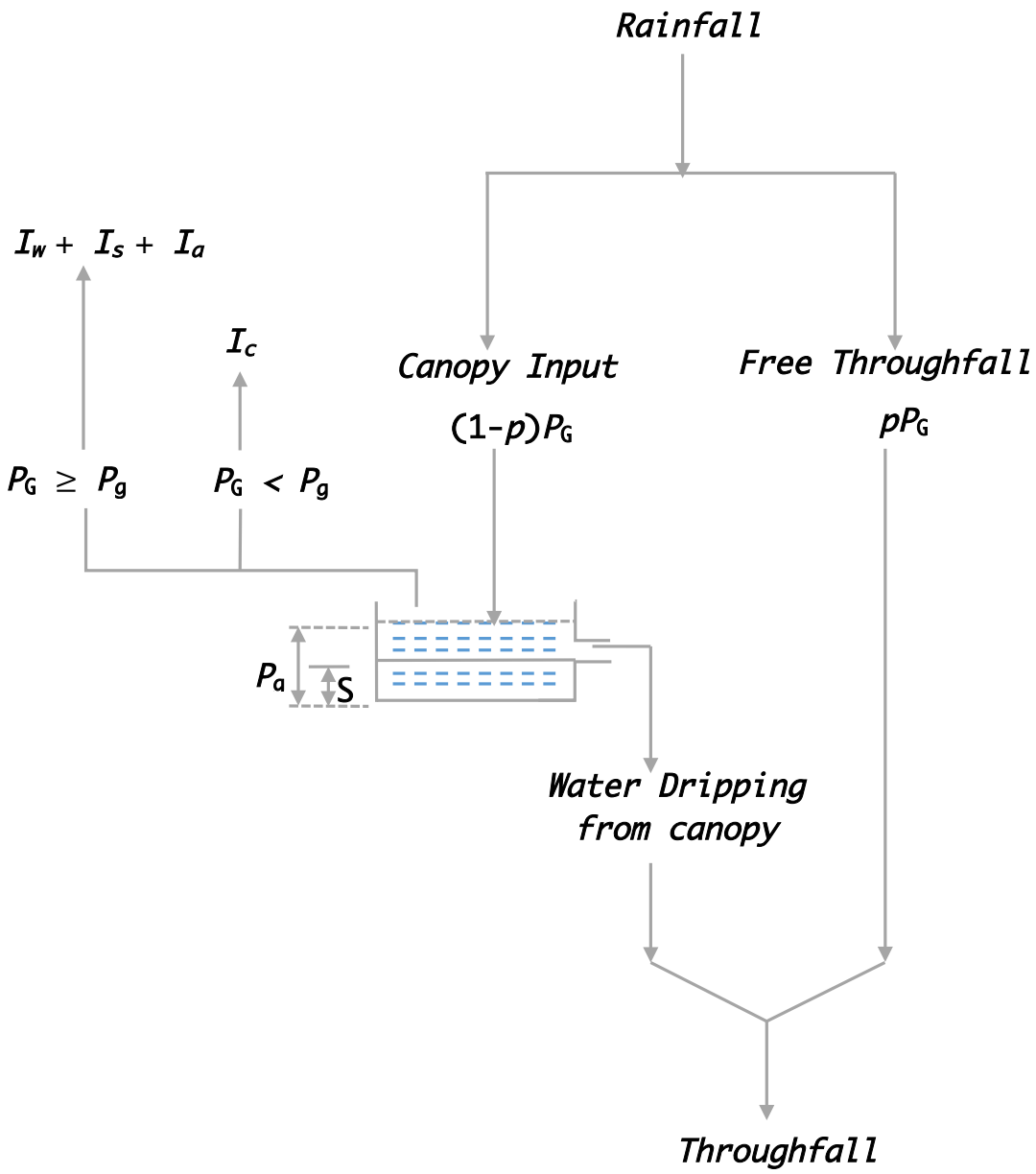

Figure 3. Conceptual framework of the interception components in the Gash model (modified from Gash and Morton, 1978).

Based on above illustration, the calculations of interception components were developed as follows (Link et al., 2004):

For m small storms insufficient to saturate the canopy (i.e. $P_G < P_g$), the amount of interception (I_c) is computed as:

$$I_c = (1-p)\sum_{j=1}^{m} P_{G,j} \quad (6)$$

For n large storms sufficient to saturate the canopy (i.e. $P_G \geq P_g$), there are three stages of interception involved:

1) Interception (I_w) during wetting up of the canopy (i.e. before saturation):
$$I_w = n(1-p)P_g - nS \quad (7)$$

2) Evaporation during canopy saturation (I_s):
$$I_s = (\frac{\bar{E}}{\bar{R}})\sum_{j=1}^{n}(P_{G,j} - P_g) \quad (8)$$

3) Evaporation after rainfall ceases (I_a): (assuming no water dripping from the canopy after the rain stops)
$$I_a = nS \quad (9)$$

Total net interception loss:
$$I_{net} = I_c + I_w + I_s + I_a \quad (10)$$

The mean amount of rainfall required to saturate the canopy (P_g) that applied in Link et al. (2004) and was originally derived from Gash (1979) assuming no water dripping from the canopy before saturation, and is given by:
$$P_g = -\frac{\bar{R}S}{\bar{E}}\ln\left[1 - \frac{\bar{E}}{\bar{R}(1-p)}\right] \quad (11)$$

Chapter 3. Model Evaluation

3.1 Model Performance

Before testing the model on four selected broadleaf species, it was validated by comparing the results of modelled throughfall with actual measured throughfall data. The model was applied on an event basis using both *T*-P_G estimated $\bar{E}/\bar{R}$ (Figure 2), and the Penman-Monteith equation estimated $\bar{E}/\bar{R}$ (Table 1). The throughfall data for species of interest in this study was not available, thus throughfall data for one single Douglas-fir tree and one single Western red cedar tree measured by Asadian and Weiler (2009) over a one-year period were used. *S* and *p* for both

approaches of estimation of $\bar{E}/\bar{R}$ were obtained from the $T - P_G$ plot. The interception loss for each of Douglas-fir and Western red cedar was obtained by applying the same method of calculation described in Section 2.2.3. The modelled throughfall results were then obtained by applying Equation (1).

Figure 4a and Figure 4b show the comparison of the two approaches of modelled throughfall and measured throughfall for a single tree of Western red cedar and Douglas-fir, respectively. Overall, the model performs relatively well, and the difference between the two $\bar{E}/\bar{R}$ estimation approaches is minimum. The model slightly overestimates the throughfall (i.e. underestimating the interception) for both applied approaches. Nevertheless, the pattern of modelled and measured throughfall mimics each other quite well (Figure 4a; 4b). $\bar{E}/\bar{R}$ estimated using the T-P_G plot shows less overestimation on throughfall compared to Penman-Monteith estimated $\bar{E}/\bar{R}$ (Table 2). For both species, the modelled and measured data start diverging in the month of April. In the month of October, the modelled and measured data for Douglas-fir starts merging, while the difference between modelled and measured data increases in the case of Western Red Cedar.

Many factors could cause differences between modelled and measured data. Differences in crown shape and leaf morphology of Western red cedar and Douglas-fir lead to variations in rainfall distribution patterns and the total amount of throughfall reaching the ground. Any discrepancy between modelled and measured interception losses derive from uncertainty, not only of the canopy characteristics, but also of the variations in rainfall rates and evaporation rates. High evaporation rates in summer months and larger variances of rainfall rates in late fall and winter months impact the total interception losses for these two species. More importantly, the rainfall rate and evaporation rate should be measured specifically for complete canopy saturation condition during a rainfall event, as the Gash model is very sensitive to these two parameters (Asdak et al., 1998; Pereira et al., 2009). In the case of this comparison, $\bar{E}/\bar{R}$ obtained from both approaches were treated as constants over the event period rather than the period after complete saturation conditions. Assuming $\bar{E}/\bar{R}$ is constant during a rainfall event may not be appropriate, especially during the wetting phase and is potentially responsible for introduced errors (Link et al., 2004). Additionally, treating S and p as constants is also questionable, as they can be affected by moisture, temperature and evaporation rate (Véliz-Chávez et al., 2014). It should be remembered that the

model summarizes general conditions. Minor disagreements are reasonable, as the measured data only represent the interception loss of one tree species for one rainfall event.

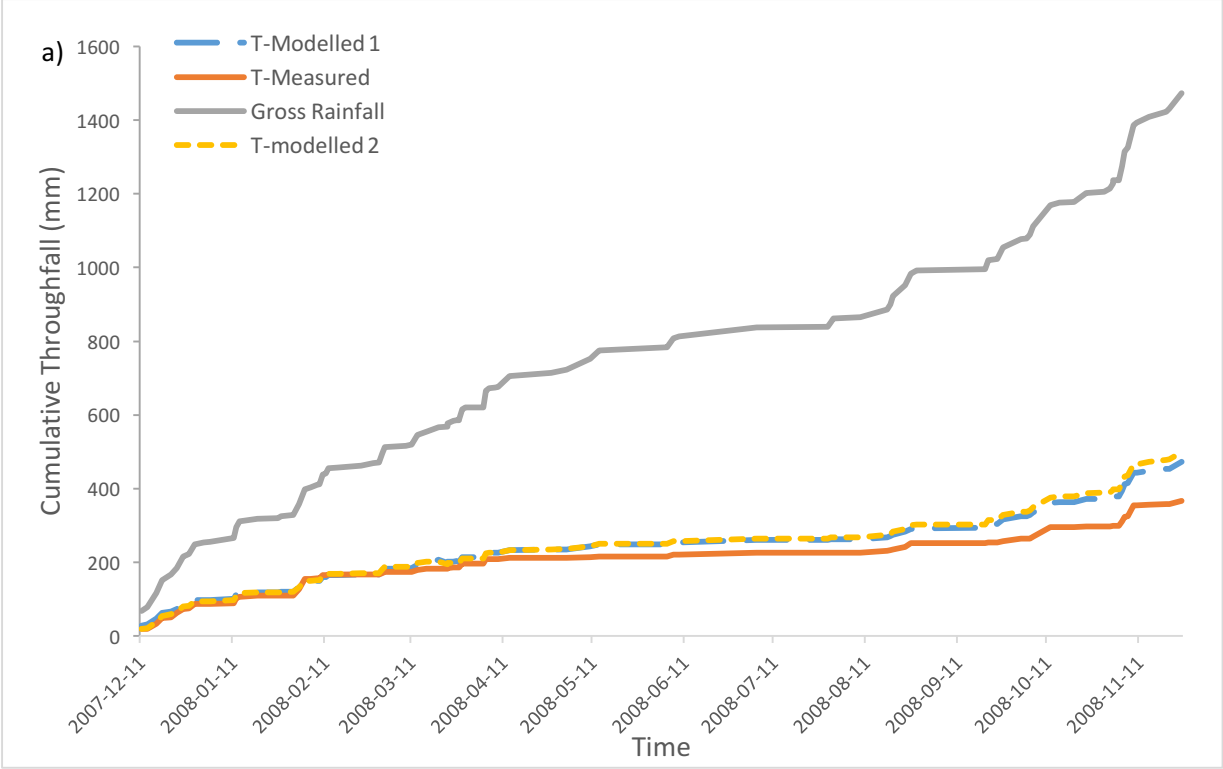

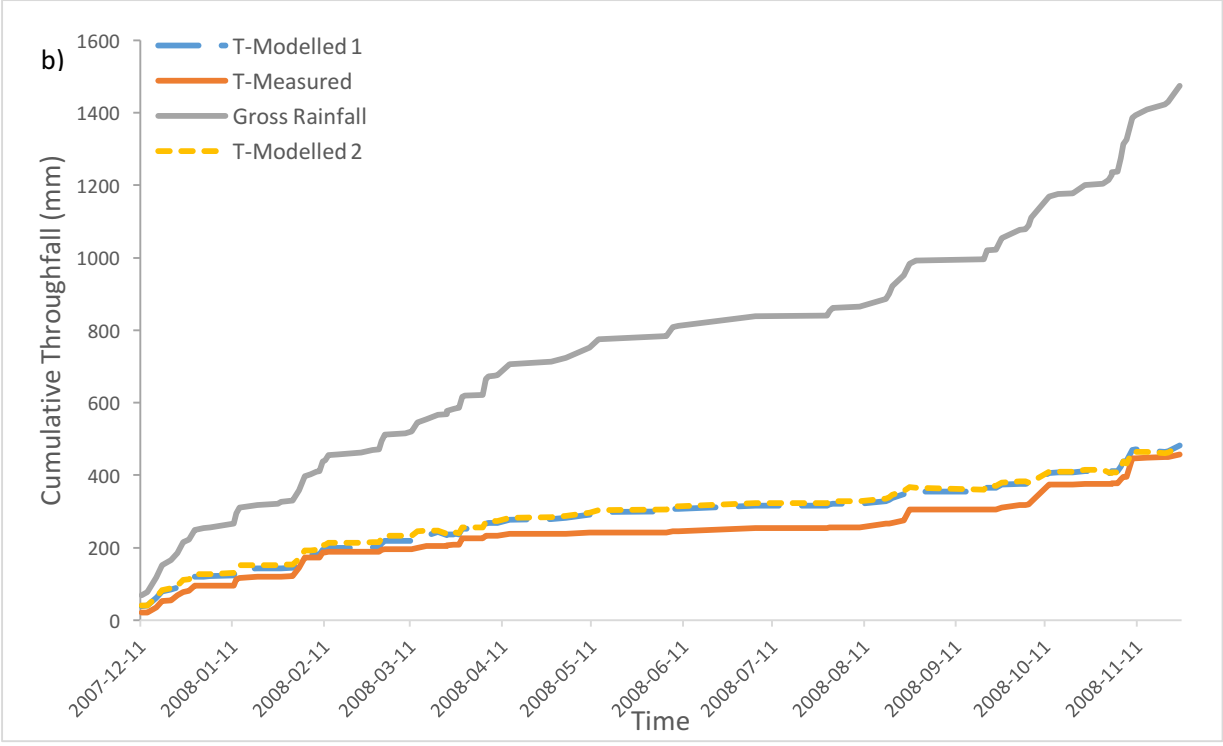

Figure 4. Cumulative rainfall (P_G) and throughfall (T) for two species: a) Western red cedar (WRC); b) Douglas Fir (DF). Both measured and modelled throughfall are presented (T-modelled 1: T-P_G estimated $\bar{E}/\bar{R}$; T-modelled 2: Penman-Monteith equation estimated $\bar{E}/\bar{R}$).

Table 2. Results of the comparison of modelled and measured throughfall for two species.

	Western red cedar		**Douglas fir**	
	$T - P_G$ estimated $\bar{E}/\bar{R}$	Penman-Monteith estimated $\bar{E}/\bar{R}$	$T - P_G$ estimated $\bar{E}/\bar{R}$	Penman-Monteith estimated $\bar{E}/\bar{R}$
P_G (mm)	1473.66	1473.66	1473.66	1473.66
T (mm) measured	366.04	366.04	457.59	457.59
T (mm) modelled	472.73	498.96	480.70	482.30
Normalized averaged error (%) for modelled interception loss	22.57%	26.64%	4.81%	5.12%

3.2 Sensitivity Analysis

Although the model performance is influenced by the combination effects of all parameters, some parameters do have stronger impacts than the others. In practical applications, obtaining parameters that meet all requirements is challenging and often constrained by limited time and resources. Knowing the parameter that has the most significant impacts on the model would benefit model users by prioritizing efforts on the most important factors. Therefore, a sensitivity analysis was conducted on the three major parameters in the model (i.e. S, p, $\bar{E}/\bar{R}$) using the mean, minimum, and maximum values of each of the parameters obtained from Link et al. (2004). In this analysis, the variation of S ranged from 2.7 to 4.3 mm; p ranged from 0.03 to 0.73; $\bar{E}/\bar{R}$ ranged from 0.02 to 0.38 (Link et al., 2004).

Figure 5a, 5b, and 5c illustrate the results of the sensitivity analysis for each of $\bar{E}/\bar{R}$, p, and S. Among the three major parameters, the $\bar{E}/\bar{R}$ ratio is the most influential parameter in the model (Figure 5a). A similar result was found in Šraj et al. (2008), who indicated a 10% change in $\bar{E}/\bar{R}$ leads to a 7% change in the modelled interception loss. In Figure 5a, the pattern of cumulative interception was amplified by the maximum value and smoothed out by the minimum value of

$\bar{E}/\bar{R}$. It would be intriguing to know which one of $\bar{E}$ and $\bar{R}$ has a more significant impact on the model results. Unfortunately, with the current accessibility of data, it was not possible to separate the effect of $\bar{E}$ and $\bar{R}$. The impacts of maximum and minimum $\bar{E}/\bar{R}$ ratio could be explained to some extent by allowing $\bar{E}$ or $\bar{R}$ approach an extreme value. It is estimated that $\bar{R}$ has more significant impacts on the model than $\bar{E}$ by looking at the effects of maximum and minimum value of $\bar{E}/\bar{R}$ ratio (Figure 5a). Xiao et al. (2000) reported that the interception loss could increase from 32% to 57% with a reduction of 50% in rainfall rate for an oak tree. Decreasing rainfall rate reduced the amount of rainwater added to the tree canopy, resulting in the accumulation of a large proportion of rainwater used for wetting the crown surface (Xiao et al., 2000).

Compared to $\bar{E}/\bar{R}$, the model shows less sensitivity to both p and S. Gash and Morton (1978) reported that a change of 50% in S leads to a variation in interception loss of 15%, and a change of 50% in p leads to 7% difference in interception loss. However, in this comparison, more significant impacts were observed with the maximum value of p (Figure 5b). The maximum applied p value leads to a higher degree of departure from originally modelled value. A maximum at 0.73 of p means that 73% of rainfall on the tree directly reaches the ground without touching leaves and branches, which would imply only minimum canopy cover in this case. A similar maximum value of p during the leafless period was found in Šraj et al. (2008). And only minor impacts were observed with variations in S (Figure 5c). Higher impacts of S compared to p was also reported by Šraj et al. (2008), who indicated a 10% change in S results in a change of 1.4% in modelled interception and only 0.8% for the same percentage change in p. The influences of canopy parameters should be restricted to the period of canopy wetting up and the amount of water left on the canopy after rainfall has ceased (Gash and Morton, 1978), as shown in Equation (7) and (9). Low sensitivity of canopy parameters for this analysis could also reflect the rainfall and evaporation characteristics over this study period.

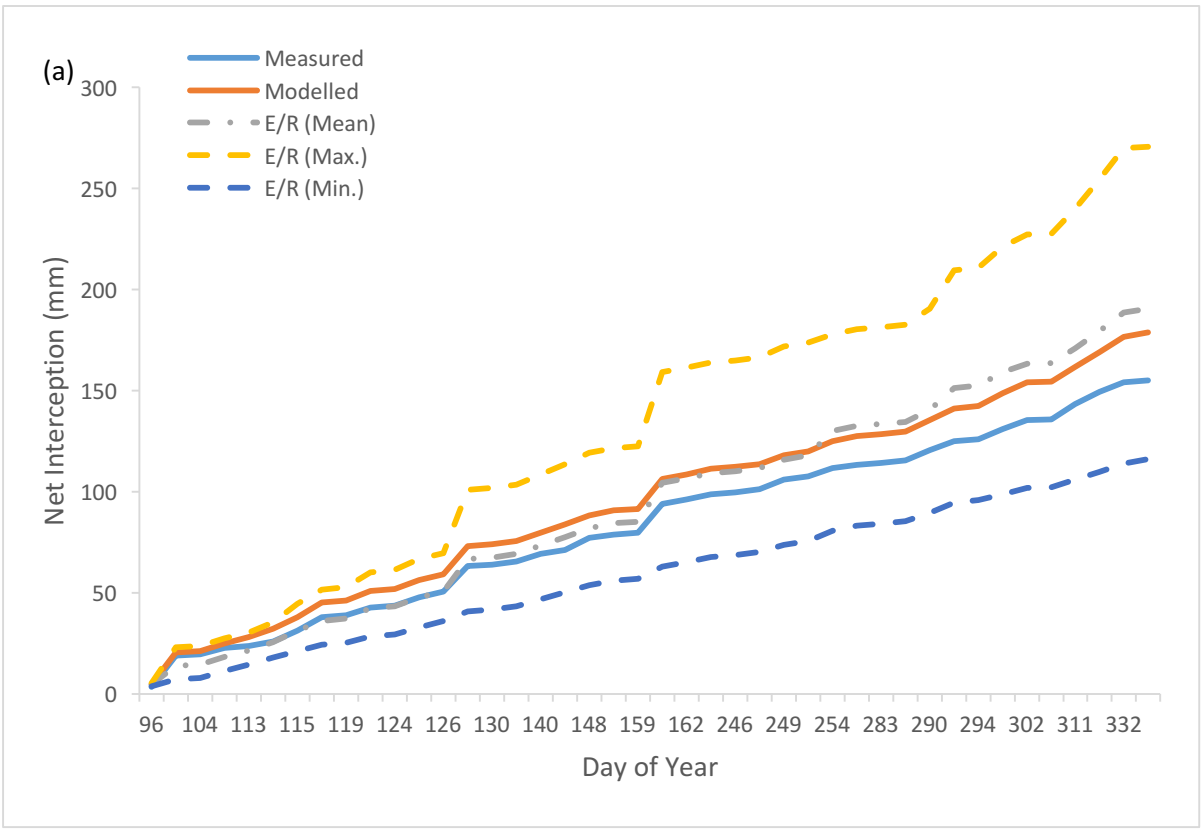
(a)
Measured
Modelled
E/R (Mean)
E/R (Max.)
E/R (Min.)
Net Interception (mm)
300
250
200
150
100
50
0
96 104 113 115 119 124 126 130 140 148 159 162 246 249 254 283 290 294 302 311 332
Day of Year

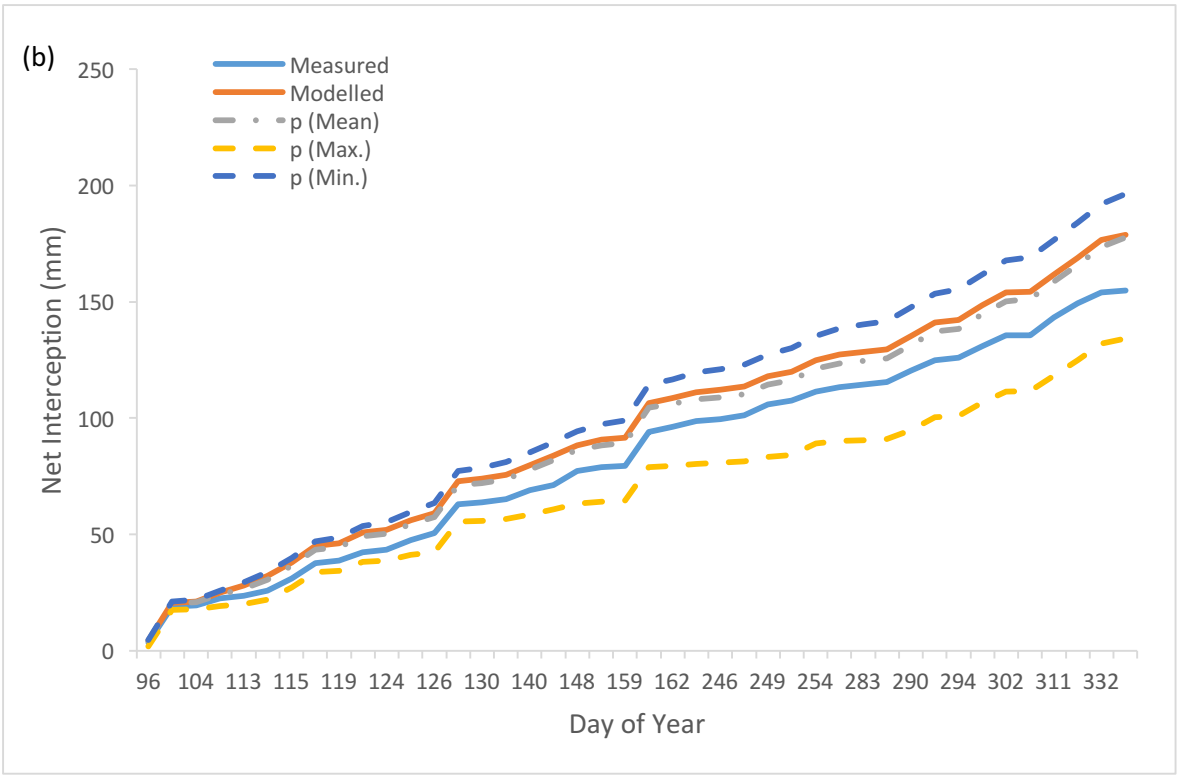
(b)
Measured
Modelled
p (Mean)
p (Max.)
p (Min.)
Net Interception (mm)
250
200
150
100
50
0
96 104 113 115 119 124 126 130 140 148 159 162 246 249 254 283 290 294 302 311 332
Day of Year

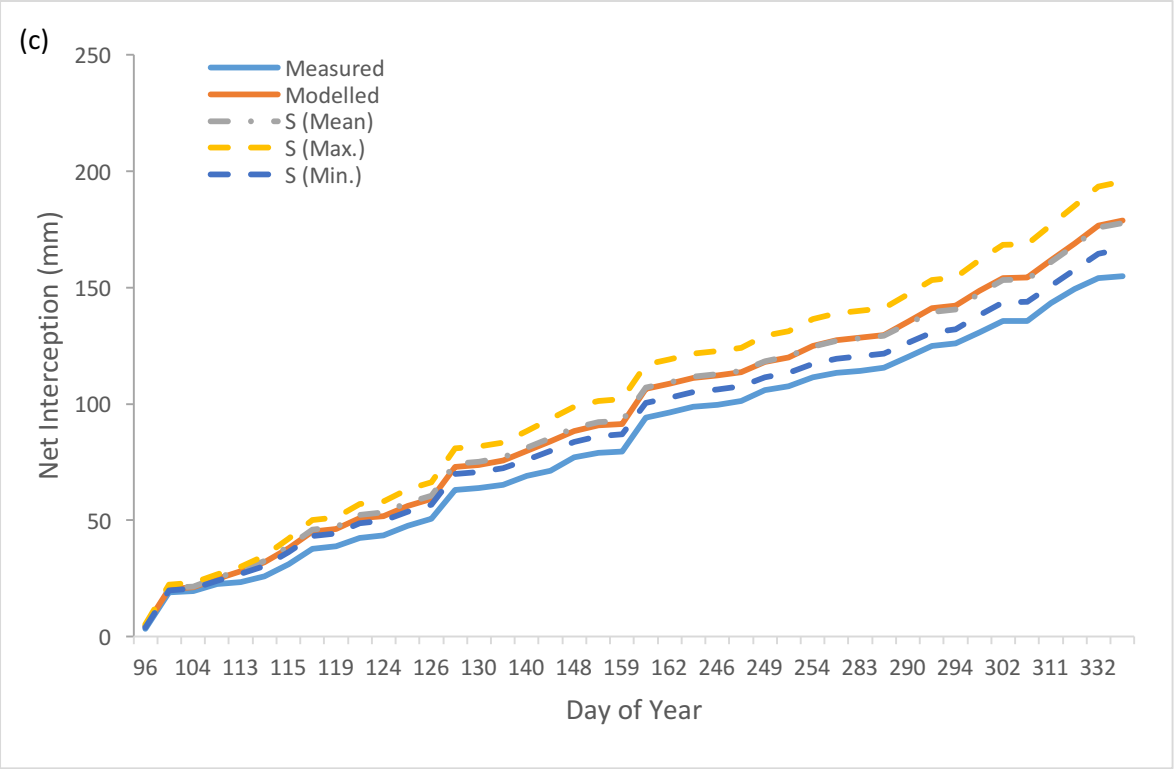

Figure 5. Sensitivity analysis for a) $\bar{E}/\bar{R}$, b) p, and c) S with the mean, maximum, and minimum values applied.

Chapter 4. Model Application to Four Tree Species

Chapter 3 demonstrated that the Gash analytical model of canopy interception is an effective tool to estimate interception loss. To see how the interception performance varies among deciduous trees, it would be preferable to test it against the tree species that are grown in local municipalities. However, the throughfall data for interested species is not available in this study to allow the estimation of $\bar{E}/\bar{R}$ using T-P_G method. Thus, the Penman-Monteith estimated $\bar{E}/\bar{R}$ was used for this test. The tree selection was determined by a simple survey conducted among several local municipalities, namely the District of North Vancouver, the District of Kent, Agassiz, the City North Vancouver, the City of Maple Ridge, the City of Surrey, the City of Coquitlam, the City of New Westminster, the City of Port Moody, and the Township of Langley. White Oak (*Quercu alba L.*), Norway maple (*Acer platanoides L.*), Green ash (*Fraxinus pennsylvanica Marsh.*), and

Prunus spp. are among the most common planted street tree species in these urban areas, and were thus selected for the rainfall interception model.

4.1 Overview of Meteorological data

The climate data from December 2007 to November 2008 are given in Figure 6. These data were acquired from the climate station located at Vancouver International Airport, British Columbia (Environment Canada, 2015). Data show that the highest amount of precipitation occurred during November and March in 2008, and the highest mean daily temperatures were observed in the months of July and August. For this analysis, the seasons were divided as winter (Dec, Jan, Feb), spring (March, April, May), summer (June, July, Aug), and fall (Sept, Oct, Nov).

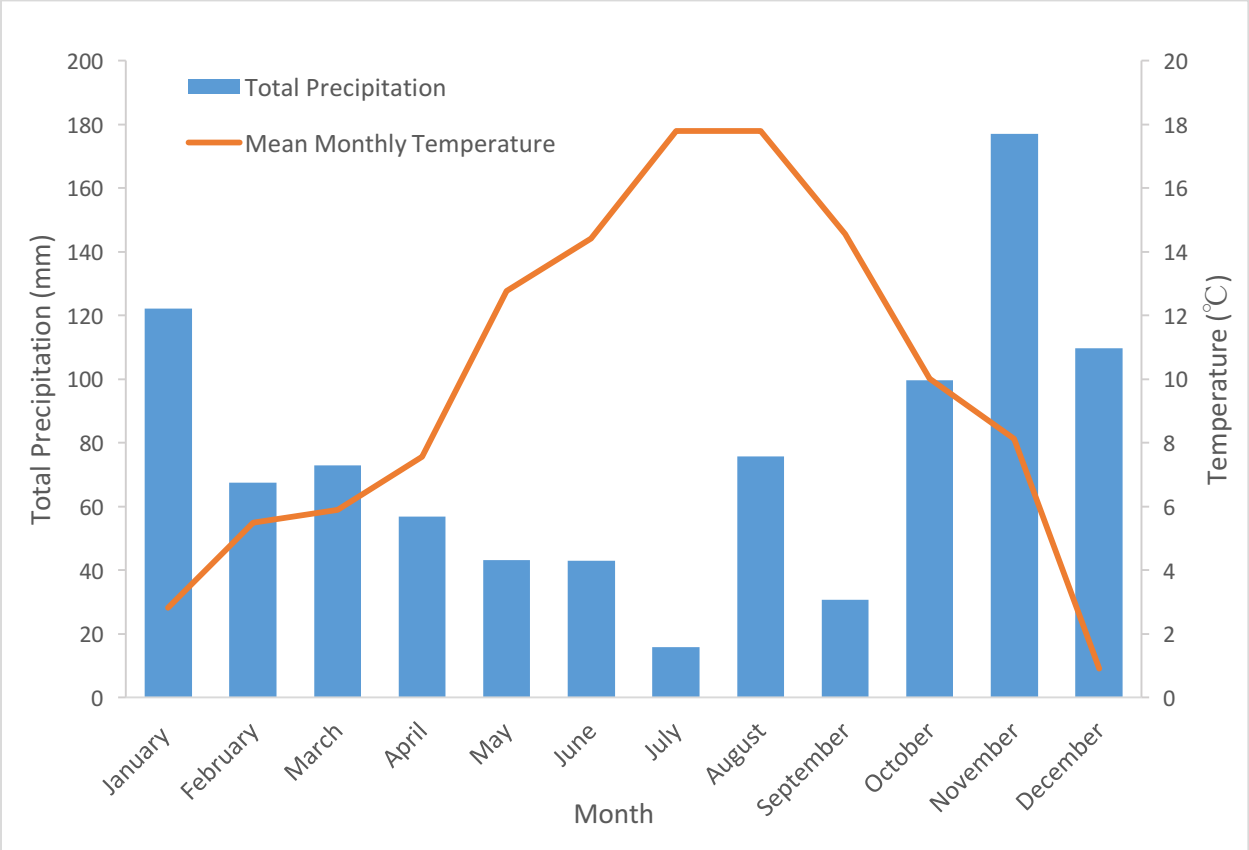

Figure 6. Vancouver's Climate Data from December 2007 to November 2008 (Location of rain gauge: Latitude 49°11'42N; Longitude: 123°10'55 W)

4.2 Seasonal rainfall interception performance

Figure 7a shows the results of the modelled interception loss of the four selected deciduous species. Because all four species were assumed to lose their leaves during winter, the storage of the trees

was dominated by stem and branches. Thus the rainfall interception performances are the same for all selected species in the winter months (Figure 7a). The cumulative rainfall intercepted by each species diverged in March and April. Among the four species, White oak showed the highest capacity of interception through the whole study period, followed by Norway maple, Green ash, and *Prunus spp*., and only minimum differences were observed between Green ash and *Prunus spp*. Differences in water storage capacities among these species reflected the differences in the morphogenesis of leaf surfaces, which influence the surface water storage, by affecting the amount of throughfall and drop-size (Xiao and McPherson, 2016). For example, Green ash has compound leaves with flexible leaflets, and the length of each leaf blade ranges from 5-10cm. In contrast, White oak has a larger leaf size (10-20cm) with lobed leaf margin (Figure 8). Other factors varied among species, such as leaf hydrophobicity, roughness, geometry, and inclination, which also have impacts on the water storage capacity of the leaf surface (Nanko et al., 2006; 2013). Despite the difference among species, the patterns of cumulative interception for each species are almost parallel to each other until the late summer, where larger divergences among species were observed.

Figure 7b shows averaged interception loss, per event, on a monthly basis for each species. All four species present similar monthly pattern of interception capacity. In general, a high peak for all species was observed in summer months, and the lowest interception loss was observed in the winter months, where only minor rainfall was intercepted by the stem and the branches for all species. The averaged interception loss for each rainfall event in spring started at 1.42mm and 1.14mm for White oak and Norway maple, respectively, and gradually increased over time. June received the highest interception loss for all species. High interception loss per rainfall event during summer could be explained by the high evaporation rate controlled by the air temperature. It is evident that annual patterns of air temperature (Figure 6) and average interception loss (Figure 7b) are similar during spring and early summer, but variations were observed in late summer and fall. Although evaporation rate is a critical factor affecting interception loss, rainfall rate can alter the interception pattern when large variations come into play. The amount of rainfall received in fall and winter in Vancouver area are high, consequently leading to more significant variations of rainfall rate compared to that in spring and summer.

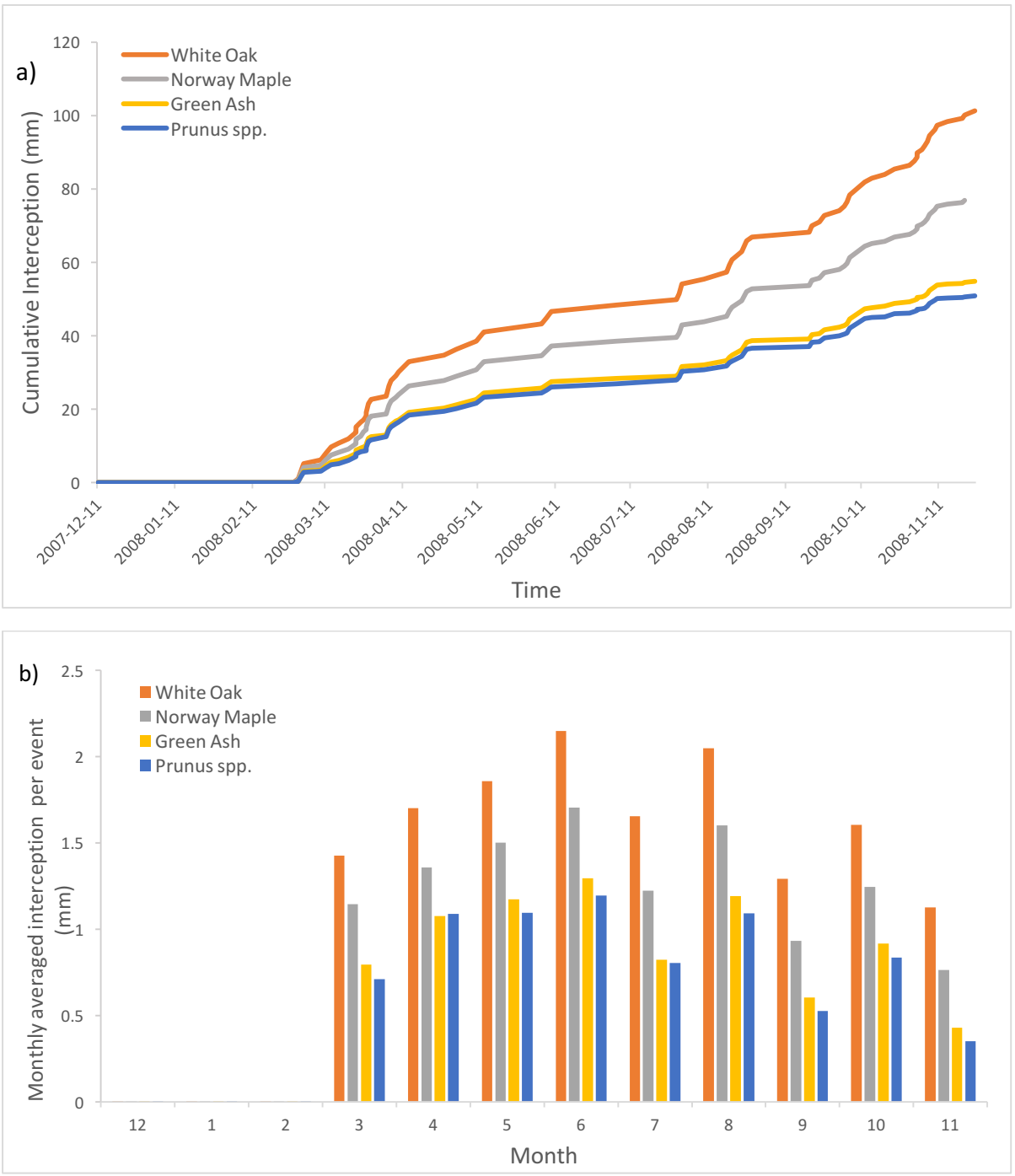

Figure 7. Seasonal interception loss of four tree species (White Oak, Norway Maple, Green Ash and *Prunus spp*.), presented as: a) cumulative sum of interception loss, and b) monthly averaged interception loss for each rain event.

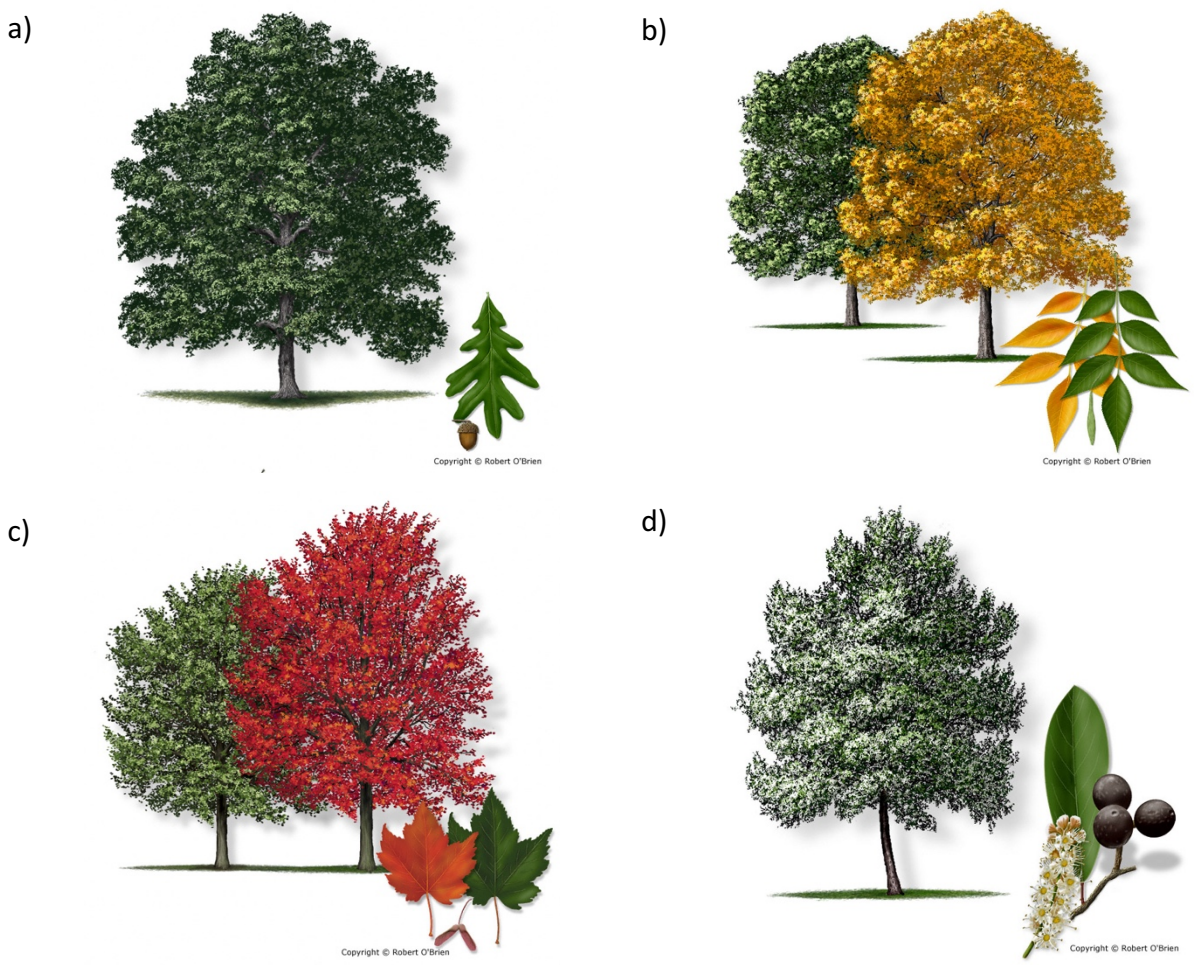

Figure 8. Tree crown and leaf morphology of sample tree species: a) White Oak; b) Green ash; c) Red maple (*Acer rubrum*); 4) Cheery-Laural (*Prunus caroliniana*) (Texas A&M Forest Service, 2014)

4.3 Future Interception Performance

Global climate models (Pacific Climate Impacts Consortium, 2013) have indicated that increasing temperatures, changing precipitation patterns, and more frequent and severe extreme weather events are likely to be observed in the District of North Vancouver in the near future. Data shows that the average annual temperature in the District of North Vancouver is expected to increase by 2.9°C with the greatest increase of 3.6°C in summer months by 2050s (Appendix B). In particular, summer maximum temperatures are expected to increase by 3.9°C, while winter minimum temperatures may warm by 5.1°C. Meanwhile, the annual precipitation is projected to increase a modest amount of 5% in District of North Vancouver by 2050s. Rainfall in winter, spring, and fall

are expected to increase between 4% and 11%. Increasing rainfall could potentially increase the amount of stormwater that must be considered at any one event, thus increasing the challenges in stormwater management, which is among the top concerns in the District of North Vancouver. Thus it is important to test out how tree species perform differently in intercepting rainfall under a changing climate.

Due to data availability, changes of temperature in the 2020s, 2050s, and 2080s were applied in the model. Figure 9 shows the trend of temperature and interception loss of White Oak, Norway maple, Western red cedar, and Douglas-fir from the current year to 2080s. Overall, no large increases in interception loss were observed. Spring and summer are found to have higher increases in interception loss compared to fall and winter. Among the four species, deciduous trees (i.e. White Oak, Norway maple) tended to have higher gains of interception loss in the fall compared to coniferous trees. No clear relationship was observed between interception and the increase of temperature, although both gently increased over time. As shown in Table 1, the temperature is one of the components in the calculation of $\bar{E}$. Changing $\bar{E}$ is expected to have more obvious impacts on the model, as explained in the sensitivity analysis (Figure 5a). No clear relationship between temperature and interception loss might indicate that temperature alone is a less decisive component of $\bar{E}$. As shown in Figure 10, the increase of temperature only led to a slight change in $\bar{E}$. Wind speed was shown to be more influential on interception loss by increasing evaporation (Šraj, et al., 2008), and was reported to influence *S* by changing the rainfall pathway (Xiao et al., 2000). It should be kept in mind that the interception process is controlled by more than one parameter. More consideration of data parameters would be required to conduct a full projection of future interception performance, as the change in temperature is only one among various consequences of climate change. Further investigations on other parameters or more sensitive parameters, such as $\bar{R}$, might also be needed to improve the outcomes of the current projection.

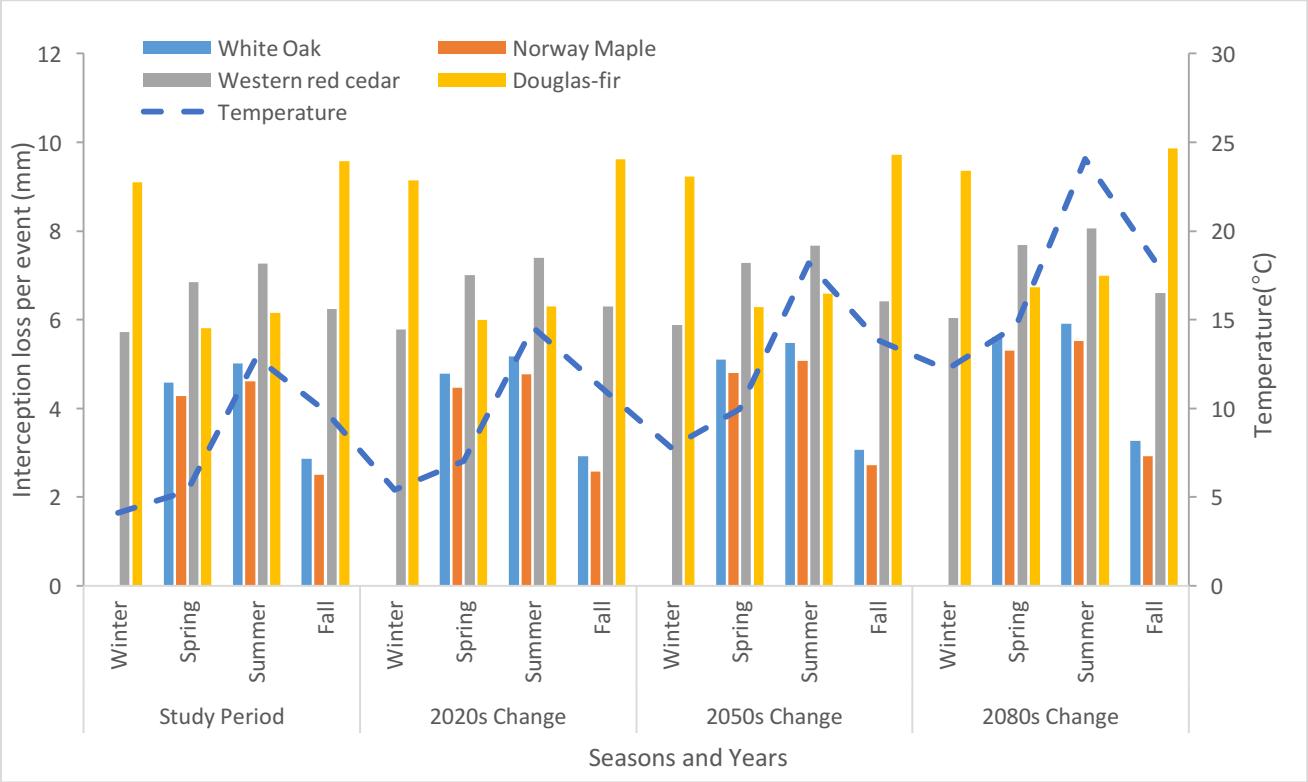

Figure 9. Projected trends of temperature and interception of four tree species (White Oak, Norway Maple, Western Red Cedar and Douglas-Fir) in the 2020s, 2050s, and 2080s, and the current study period (Dec. 2007- Nov.2008) for comparison.

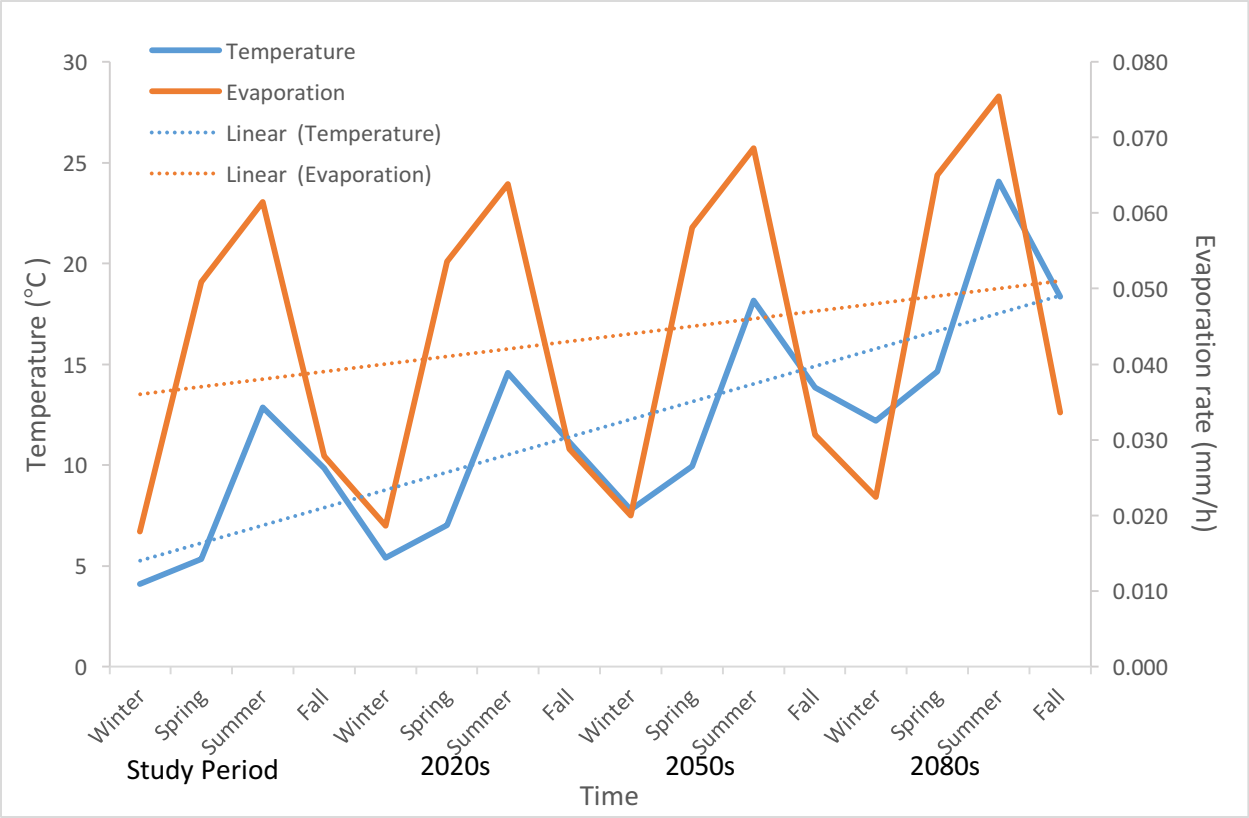

Figure 10. Relationship between temperature and evaporation rate in the study period (Dec. 2007-Nov. 2008) the 2020s, 2050s and 2080s.

Chapter 5. Limitations and Recommendations for Future Research

5.1 Limitations

Despite the satisfactory outcomes, there are a few limitations identified in this study:

- $\bar{E}/\bar{R}$, S, and p were assumed to be constant over the whole rainfall event. This assumption could lead to the discrepancy between modelled interception loss and actual interception loss as discussed in section 3.1. In fact, both $\bar{E}$ and $\bar{R}$ should correspond to the period after tree canopy is completely saturated.
- LAI values were applied from a different study area. LAI varies in different environments, even for the same tree species. For example, various types of land use could lead to different LAI values for the same species, because it measures the total leaf surface area (one side) divided by land area (Nowak et al., 2013). Deviation in LAI could cause biases

in the estimation of both S and p in this model, as S and p were derived from their relationships to LAI (Equations 4 and 5).

- Variations in leaf phenology of different species were ignored. Leaf phenology determines the timing of the emergence of leaves; the growth of leaves and leaf fall (Rodriguez et al., 2014). This model simply assumed the leaf-on season is spring, and the leaf-off season is winter for all broadleaf species, which is not true in reality. Although no dramatic changes in interception pattern were expected for the four selected species if leaf phenology were specified, the cumulative amount of interception might vary in different species.
- Spatial distribution of rainfall was ignored. Spatial distribution of rainfall affected by crown shape and wind direction were not considered in this model. If tree crown shape and wind direction were considered, the amount of rainfall interception by species might vary as these factors influence the total amount of rain and falls on crown.

5.2 Recommendations

Sensitivity analysis of the model parameters (section 3.2) and the feasibility of throughfall data measurements should be considered when implementing the rainfall interception model. Special attention should be paid to obtaining more precise values for key parameters, as they are the fundamental components to achieve satisfactory model performance. Some parameters require more time and effort than others to estimate. Recommendations to address the limitations are:

- Prioritizing efforts on obtaining $\bar{E}/\bar{R}$, if resources and time are constrained. Among the three key parameters, the model is the most sensitive to $\bar{E}/\bar{R}$. Optimizing $\bar{E}/\bar{R}$ could improve the model performance at a higher degree than the other two parameters.
- Estimation of $\bar{R}$ is critical. Special attention should be paid to the choice of method used to estimate $\bar{R}$, because it is used to determine the amount of time the canopy is saturated and should correspond to the hours when rainfall equals or exceeds a given threshold (i.e. P_g). Although it was not possible to test the impact of $\bar{R}$ alone on the model in this study, sensitivity analyses suggested $\bar{R}$ tends to be more influential than $\bar{E}$ (see section 3.2).
- Measure LAI of target tree species. Commercial instruments such as LAI-2000 (LI-COR Biosciences, 2010) and AccuPAR ceptometer (Decagon Devices, 2015) are often used for LAI measurements, but these instruments can be expensive and are characterized by low portability. Alternatively, a newly developed cell phone app – Pocket LAI (Cassandra,

2014) is an innovative way to make LAI measurements. Many studies have tested the Pocket LAI on different species and reported that it is a suitable alternative to the other commercial tools for estimating LAI, especially when resources and portability are the key issues (Confalonieri et al., 2013; Francone et al., 2013; Orlando et al., 2015).

- Specify foliage months for each species. High-resolution remote sensing images could provide a relatively accurate match with the ground observation regarding the detection of green-up dates (Polgar and Primack, 2011); however, this approach could be limited by economic constraints. Leaf phenology data of some plants might be obtained at The Japanese Metrological Agency, which has been recording leaf phenology data in phenological gardens at over 100 weather stations since 1953 (Ibáñez et al., 2010). However, different growth environments could result in changes in foliage timing.

Chapter 6. Conclusion

The goal of this project was to provide an analytical model on rainwater interception performance of a selection of common urban trees in the Metro Vancouver area, given a series of climatic conditions and tree characteristics. Overall, the model performed with a reasonable capacity to simulate the interception loss and results mimicked actual observation, given limited data inputs and with stated assumptions. The discrepancy between modelled data and actual observation could be the result of a series of factors, such as air temperature, wind speed, relative humidity, leaf area index, and rainfall rate. The lack of corresponding evaporation rate and rainfall rate ratio to a saturated canopy condition often introduces errors when applied in the model. The sensitivity analysis emphasized the relative significance of evaporation rate and rainfall rate ratio, crown storage and free throughfall coefficient to the model performance. Evaporation rate and rainfall rate ratio was identified as the most influential parameter in the model. The influences of S and p on the model also depend on evaporation and rainfall characteristics. Separating the impacts of evaporation rate and rainfall rate would require more detailed sensitivity analysis. The inter-species variation on interception was evident as White Oak showed the highest interception loss in both cumulative values and monthly average values for each rainfall event. This was followed by Norway maple, Green ash, and *Prunus spp*. Leaf morphology and other factors affecting leaf surface water storage capacity are partially responsible for the inter-species variation. Measuring

seasonal variation in leaf area index is recommended to enhance the estimation of crown storage and free throughfall coefficient. The influence of air temperature alone on this model was not as obvious as expected, as the assessment of future changes of air temperature in this model did not show a clear pattern of variation on four tested species.

As urbanization proceeds, extensive areas of vegetated landscape will be replaced by urban development. If the new urban developments are not well-designed, the area of impervious surfaces will increase and potentially aggravate current challenges with stormwater management and flooding. In the District of North Vancouver, stormwater management is a priority, especially during the wet winter season. Utilizing trees in new developments, as a core green infrastructure component, can augment stormwater conveyance (grey) infrastructure, and provide additional benefits such as cooling effects, net carbon emission reduction, and air quality improvement. This initial version of the rainfall interception model provides useful information to address several aspects of urban stormwater management for different stakeholders. It supports the process by which the amount of stormwater runoff can be reduced and delayed by urban trees, as well as the stormwater management costs that are potentially avoided by planting urban trees. Such information could be utilized by city planners, engineers and decision makers in the assessment of urban trees' benefits and the development of stormwater management plans. The results of the model also assist tree species selection regarding their interception capacity, which would offer options for developers and landscape architects in selecting specific tree species to fit various goals. A full guideline of tree species selection considering broad aspects of urban trees' benefits and its adaptation to climate change is provided in the *Urban Forest Climate Adaptation Framework for Metro Vancouver* (Diamond Head Consulting Ltd, 2016). Nonetheless, this project could serve as the basis for future research, such as a detailed sensitivity test separated impacts of evaporate rate and rainfall rate on the model, as well as on additional model parameters. The spatial distribution of rainfall associated with wind direction or crown shapes of different species could also be incorporated into future research.

Literature Cited

Asadian, Y., & Weiler, M. (2009). A new approach in measuring rainfall interception by urban trees in coastal British Columbia. *Water quality research journal of Canada*, *44*(1), 16.

Asdak, C., Jarvis, P. G., & Gardingen, P. V. (1998). Modelling rainfall interception in unlogged and logged forest areas of Central Kalimantan, Indonesia. *Hydrology & Earth System Sciences*, *2*, 211–220.

Bryant, M. L., Bhat, S., & Jacobs, J. M. (2005). Measurements and modeling of throughfall variability for five forest communities in the southeastern US, *312*, 95–108. http://doi.org/10.1016/j.jhydrol.2005.02.012

Cassandra. (2014). Pocket LAI. Retrieved from: http://www.cassandralab.com/mobiles/1

Confalonieri, R., Foi, M., Casa, R., Aquaro, S., Tona, E., Peterle, M., … Acutis, M. (2013). Development of an app for estimating leaf area index using a smartphone. Trueness and precision determination and comparison with other indirect methods. *Computers and Electronics in Agriculture*, *96*, 67–74. http://doi.org/10.1016/j.compag.2013.04.019

Decagon Devices, Inc. (2015). ACCUPAR LP-80. Retrieved from: http://www.decagon.com/en/canopy/canopy-measurements/accupar-lp-80/

Diamond Head Consulting Ltd. (2016). Urban Forest Climate Adaptation Framework for Metro Vancouver. Retrieved from: http://www.metrovancouver.org/services/regional-planning/PlanningPublications/UrbanForestClimateAdaptationFrameworkTreeSpeciesSelection.pdf

Environment Canada. (2015). Historical Data. Retrieved from: http://climate.weather.gc.ca/historical_data/search_historic_data_e.html

Francone, C., Pagani, V., Foi, M., Cappelli, G., & Confalonieri, R. (2014). Comparison of leaf area index estimates by ceptometer and PocketLAI smart app in canopies with different structures. *Field Crops Research*, *155*, 38–41. http://doi.org/10.1016/j.fcr.2013.09.024

Gash, J. H. C. (1979). An analytical model of rainfall interception by forests. *Quarterly Journal of the Royal Meteorological Society*, *105*(443), 43-55.

Gash, J. H. C., & Morton, A. J. (1978). An application of the Rutter model to the estimation of the interception loss from Thetford Forest. *Journal of Hydrology*, *38*(1-2), 49–58. http://doi.org/10.1016/0022-1694(78)90131-2

Gash, J. H., Lloyd, C. R., & Lachaud, G. (1995). Estimating sparse forest rainfall interception with an analytical model. *Journal of Hydrology*, *170*(1-4), 79–86. http://doi.org/10.1016/0022-1694(95)02697-N

GreenBlue Urban. (2016). Benefits of Urban Trees: A guide by GreenBlue Urban. Retrieved from: http://www.greenblue.com/wp-content/uploads/2016/05/Benefits-of-Urban-Trees.pdf

Ibáñez, I., Primack, R. B., Miller-Rushing, A. J., Ellwood, E., Higuchi, H., Lee, S. D., … Silander, J. A. (2010). Forecasting phenology under global warming. *Philosophical Transactions of the Royal Society of London. Series B, Biological Sciences*, *365*(1555), 3247–60. http://doi.org/10.1098/rstb.2010.0120

Klaasen, W., Bosveld, F., & de Water, E. (1995). Water storage and evaporation as constituents of

rainfall interception. *Journal of Hydrology*, *212-213*, 36–50. http://doi.org/10.1016/S0022-1694(98)00200-5

LI-COR Biosciences. (2010). Using LAI-2200 in Sunny Conditions. Retrieved from: http://www.licor.com/env/newsline/tag/lai-2000/

Link, T. E., Unsworth, M., & Marks, D. (2004). The dynamics of rainfall interception by a seasonal temperate rainforest. *Agricultural and Forest Meteorology*, *124*(3-4), 171–191. http://doi.org/10.1016/j.agrformet.2004.01.010

Liu, S. (1998). Estimation of rainfall storage capacity in the canopies of cypress wetlands and slash pine uplands in north-central Florida. *Journal of Hydrology*, *207*(1-2), 32–41. http://doi.org/10.1016/S0022-1694(98)00115-2

Leyton, L., Reynolds, E. R. C., & Thompson, F. B. (1967, September). Rainfall interception in forest and moorland. In *International symposium on forest hydrology* (Vol. 163, p. 168). Pergamon Press, New York, USA.

Maas, J., Verheij, R. A., Vries, S. De, Spreeuwenberg, P., Schellevis, F. G., & Groenewegen, P. P. (2009). Morbidity is related to a green living environment. *Journal of Epidemiology and Community Health, 63*(12), 967–973. doi:10.1136/jech.2008.079038

Maller, C., Townsend, M., Pryor, A., Brown, P., & St Leger, L. (2006). Healthy nature healthy people: contact with nature as an upstream health promotion intervention for populations. *Health Promotion International, 21*(1), 45–54. doi:10.1093/heapro/dai032

McPherson, E. G., & Simpson, J. R. (2002). A comparison of municipal forest benefits and costs in Modesto and Santa Monica, California, USA. *Urban Forestry & Urban Greening*, *1*(2), 61-74.

McPherson, G. E., Nowak, D. J., & Rowntree, R. A. (1994). Chicago's urban forest ecosystem: results of the Chicago Urban Forest Climate Project.

McPherson, E. G., van Doorn, N., & de Goede, J. (2016). Structure, function and value of street trees in California, USA. *Urban Forestry and Urban Greening*, *17*, 104–115. http://doi.org/10.1016/j.ufug.2016.03.013

Murakami, S. (2007). Application of three canopy interception models to a young stand of Japanese cypress and interpretation in terms of interception mechanism. *Journal of Hydrology, 3-4,* 305–319. http://doi.org/10.1016/j.jhydrol.2007.05.032

Nanko, K., Hotta, N., & Suzuki, M. (2006). Evaluating the influence of canopy species and meteorological factors on throughfall drop size distribution. *Journal of Hydrology*, *329*(3-4), 422–431. http://doi.org/10.1016/j.jhydrol.2006.02.036

Nanko, K., Watanabe, A., Hotta, N., & Suzuki, M. (2013). Physical interpretation of the difference in drop size distributions of leaf drips among tree species. *Agricultural and Forest Meteorology*, *169*, 74–84. http://doi.org/10.1016/j.agrformet.2012.09.018

National Aeronautics and Space Administration (NASA). (2016) Prediction of Worldwide Energy Resource (POWER). Retrieved from: http://power.larc.nasa.gov/cgi-bin/hirestimeser.cgi

Nesbitt, N. H. L., Cowan, S. B. J., Cheng, Z. C., PI, S. S., & Neuvonen, J. (2015). The Social and Economic Values of Canada's Urban Forests: A National Synthesis.

Nowak, D. J., Hoehn, R. E. I., Bodine, A. R., Crane, D. E., Dwyer, J. F., Bonnewell, V., & Watson, G. (2013). Urban Trees and Forests of the Chicago Region. *U.S. Forest Service*, 1–114.

Orlando, F., Movedi, E., Paleari, L., Gilardelli, C., Foi, M., Dell'Oro, M., & Confalonieri, R. (2015). Estimating leaf area index in tree species using the PocketLAI smart app. *Applied Vegetation Science*, *18*(4), 716–723. http://doi.org/10.1111/avsc.12181

Pacific Climate Impacts Consortium (PCIC). (2013). Statistically Downscalled Climate Scenarios. Retrieved from: https://www.pacificclimate.org/data/statistically-downscaled-climate-scenarios

Peper, P. J., McPherson, E. G., Simpson, J. R., Gardner, S. L., Vargas, K. E., & Xiao, Q. (2007). New York City, New York municipal forest resource analysis.

Pereira, F. L., Gash, J. H. C., David, J. S., David, T. S., Monteiro, P. R., & Valente, F. (2009). Modelling interception loss from evergreen oak Mediterranean savannas : Application of a tree-based modelling approach, *149*, 680–688. http://doi.org/10.1016/j.agrformet.2008.10.014

Polgar, C., & Primack, R. (2011). Leaf-out dates highlight a changing climate. *Arnoldia*, *68*(4), 14-22.

Rodriguez, H. G., Maiti, R., & Sarkar, N. C. (2014). Phenology of Woody Species: a Review. *International Journal of Bio-Resource and Stress Management*, *5*(3), 436. http://doi.org/10.5958/0976-4038.2014.00595.8

Ross, J. (1975). Radiative transfer in plant communities. *Vegetation and the Atmosphere*, *1*, 13-55.

Sanders, R. A. (1986). Urban vegetation impacts on the hydrology of Dayton, Ohio. *Urban Ecology*, *9*(3), 361-376.

Šraj, M., Brilly, M., & Mikoš, M. (2008). Rainfall interception by two deciduous Mediterranean forests of contrasting stature in Slovenia. *Agricultural and Forest Meteorology*, *148*(1), 121–134. http://doi.org/10.1016/j.agrformet.2007.09.007

Texas A&M Forest Service. (2014). Trees Texas: List of Trees. Retrieved from: http://texastreeid.tamu.edu/content/listOfTrees/

Tobón Marin, C. (1999). *Monitoring and modelling hydrological fluxes in support of nutrient cycling studies in Amazonian rain forest ecosystems.* Wageningen, The Netherlands: Tropendos Foundation

Véliz-Chávez, C., Mastachi-Loza, C. A., González-Sosa, E., Becerril-Piña, R., & Ramos-Salinas, N. M. (2014). Canopy Storage Implications on Interception Loss Modeling. *American Journal of Plant Sciences*, *5*(September), 3032–3048. Retrieved from http://www.scirp.org/journal/PaperInformation.aspx?paperID=50176

Wang, J., Endreny, T. A., & Nowak, D. J. (2008). Mechanistic simulation of tree effects in an urban water balance model. *Journal of the American Water Resources Association*, *44*(1), 75–85. http://doi.org/10.1111/j.1752-1688.2007.00139.x

Water Balance Model Express. (2016). Welcome to the District of North Vancouver Water Balance Tool. Retrieved from: http://dnv.waterbalance-express.ca

Xiao, Q., & McPherson, E. G. (2003). Rainfall interception by Santa Monica's municipal urban forest. *Urban Ecosystems*, *6*(4), 291-302.

Xiao, Q., & McPherson, E. G. (2016). Surface Water Storage Capacity of Twenty Tree Species in Davis, California. *Journal of Environmental Quality*, *45*(1), 188–198. http://doi.org/10.2134/jeq2015.02.0092

Xiao, Q., McPherson, E. G., Ustin, S. L., & Grismer, M. E. (2000). A new approach to modeling tree rainfall interception. *Journal of Geophysical Research*, *105*(D23), 29-173

Appendix A

The Penman-Monteith equation calculates potential evaporation (E_p) as:

$$E_p = \frac{sA + \rho c_p D g_a}{\lambda(s + \gamma)}$$

where s is the slope of the saturated vapor pressure curve, A is the available energy flux (i.e. net radiation), ρ is the density of air, c_p is the specific heat of air at constant pressure, D is the vapour pressure deficit, g_a is the aerodynamic conductance, λ is the latent heat of vaporization of water and γ is the psychometric constant. The detailed calculations and value setting were confirmed with Dr. T.A. Black through personal communication.

Appendix B

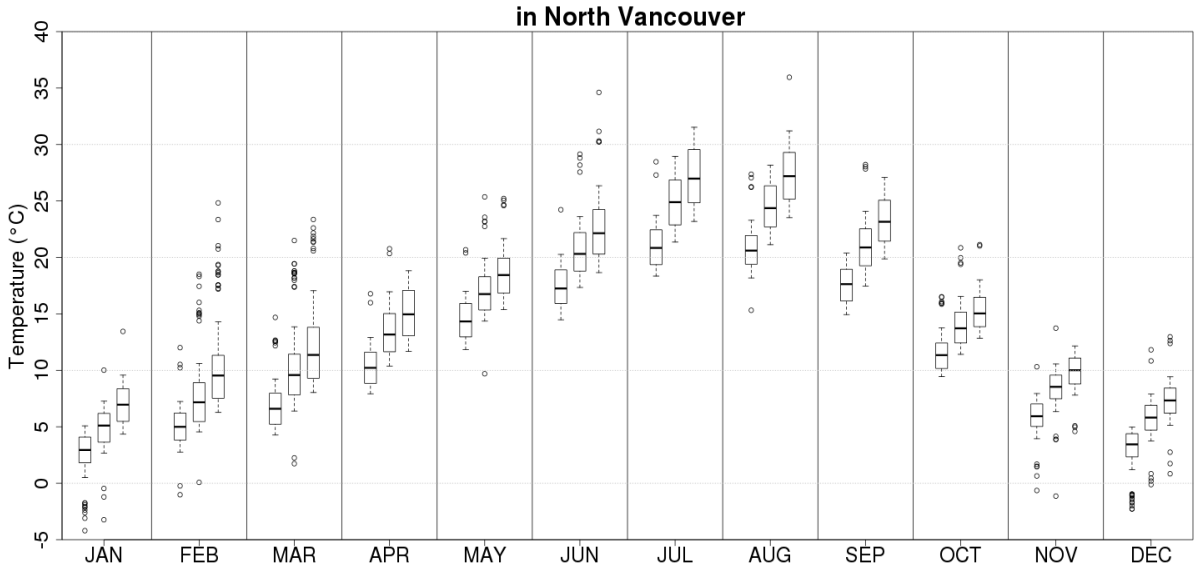

Figure A1. Seasonal variability in monthly daytime high temperatures in the DNV. In each month, boxes indicate values for the 1980s, 2050s, and 2080s, from left to right, respectively; solid lines depict median values, dotted lines represent 90th and 10th percentiles and open circles denote individual outliers.

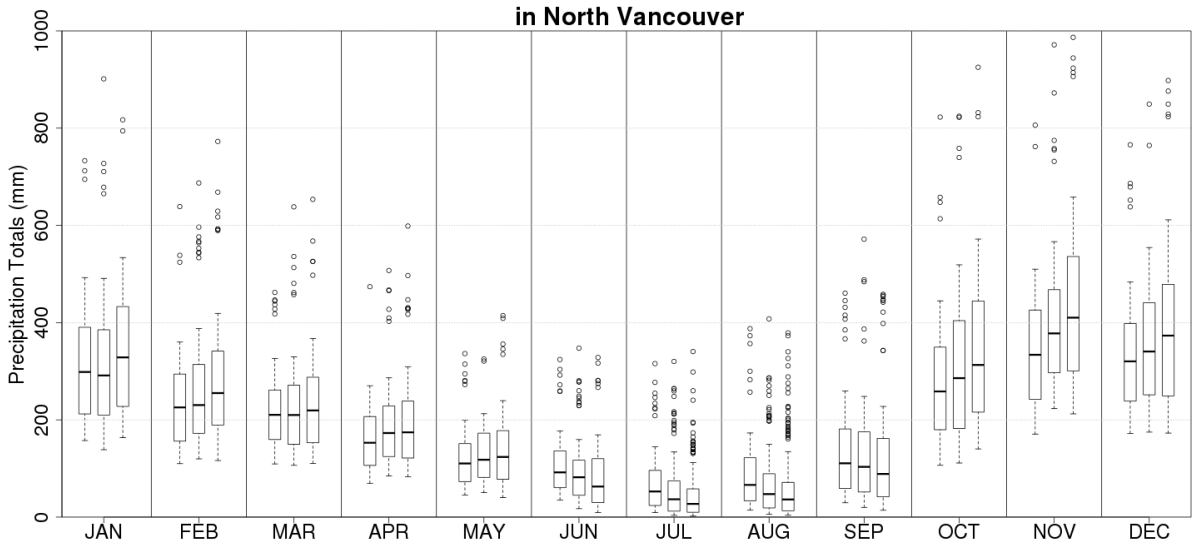

Figure A2. Seasonal variability in monthly total precipitation in the DNV. In each month, boxes indicate values for the 1980s, 2050s, and 2080s, from left to right, respectively; solid lines depict median values, dotted lines represent 90th and 10th percentiles and open circles denote individual outliers.